International Symposium
On Turbulence and Shear Flow
Phenomena (TSFP-8)
August 28 - 30, 2013 Poitiers, France

EXPERIMENTAL INVESTIGATION OF BLOWING EFFECTS ON TURBULENT FLOW OVER A ROUGH SURFACE

Mark A. Miller, Alexandre Martin and Sean C. C. Bailey
Department of Mechanical Engineering
University of Kentucky
151 Ralph G. Anderson Bldg.
Lexington, KY 40506
scbailey@engr.uky.edu

ABSTRACT

A high Reynolds number turbulent channel flow facility was used to study the combined effects of roughness and flow injection on the mean flow and turbulence characteristics. It was found that the additional momentum injection through the surface enhanced the roughness effects and for the mean flow the effect of blowing was indistinguishable from that of increased roughness. However, for the turbulence statistics, this analogy broke down in that the addition of blowing resulted in behavior which did not follow that predicted by Townsend's hypothesis. This was observed as a reduction of outer-scaled Reynolds stress well into the outer layer. The reduction in Reynolds stress was accomplished primarily by a suppression of the kinetic energy content associated with large-scale motions, which are believed to be formed at the surface but extend into the outer layer.

Introduction

Due to its influence on the wall shear stress, and hence skin friction drag, there has been considerable research effort focusing on roughness-induced turbulence (see, for example Raupach *et al.*, 1991; Jiménez, 2004), and an equal volume of effort targeting the effects of momentum injection through the surface, i.e. "blowing." (see, for example Krogstad & Kourakine, 2000; Çuhadaroğlu *et al.*, 2007). However, there are also instances where these two phenomena co-exist. For example, ablative thermal protection systems are often constructed from a carbon fiber matrix impregnated with phenolic resin. As the resin ablates due to heat flux into the thermal protection system, energy is absorbed by removal of material from the surface, thus keeping the back side of the surface at a reasonably cool temperature. The carbon matrix ablates at a much slower rate than the resin, and there results a rough surface which can trigger the transition to turbulence. Simultaneously, the ablating resin produces pyrolysis gases which emit from the surface, further modifying the turbulent boundary layer through momentum injection. Despite coexistence of roughness and momentum injection in systems such as these, very few studies have treated the combined effects of roughness and blowing boundary conditions (Healzer *et al.*, 1974; Schetz & Nerney, 1977; Voisinet, 1979; Holden *et al.*, 1988).

One of the foundational hypothesis in the studies of turbulent rough-wall flow is that of wall-similarity, or Townsend's hypothesis (Townsend, 1976), which is an extension of Reynolds number similarity for smooth walls. As summarized by Raupach *et al.* (1991), Townsend's hypothesis states that, for sufficiently high Reynolds numbers, the turbulence will be dynamically similar far from the surface and independent of wall conditions due to the numerous interactions which will occur as roughness-induced eddies are transported away from the surface. As noted by Jiménez (2004), this also implies that a limitation for wall-similarity is that the roughness height is small relative to the wall layer thickness, h (i.e. $h/k > 40$). If the roughness height exceeds this limit, the roughness will disturb the log layer and consequently roughness effects will persist into the outer layer (Jiménez, 2004; Flack *et al.*, 2004).

Using the wall-similarity argument, together with k, the roughness height, and all other length scales necessary to fully characterize the roughness, L_i, a form of the law of the wall describing the mean velocity can be derived using an asymptotic matching analysis for a rough surface as

$$U^+(y) = \frac{1}{\kappa} ln(y^+) + B - [\Delta U^+](k^+, L_i). \qquad (1)$$

Here, U is the time-averaged mean velocity, y the wall-normal distance, κ the von Kármán constant and B the additive log-law constant. The superscripted $+$ indicates scaling using 'inner variables', $U_\tau = (\tau_w/\rho)^{1/2}$ and ν , where U_τ is the friction velocity, τ_w the wall shear stress and ρ and ν the fluid density and kinematic viscosity respectively. The parameter ΔU^+ is the roughness function, representing the offset between parallel smooth and rough wall mean profiles and is a direct measure of the ability of the surface roughness to absorb momentum from the mean flow.

As with surface roughness, the effects of momentum injection or "blowing" through a surface have received significant attention due to its relevance for applications such as turbine blade transpiration cooling, flow separation control, and turbulence control. Typically, these studies focus on either blowing introduced through a slot or series of holes locally (Krogstad & Kourakine, 2000; Çuhadaroğlu *et al.*, 2007) or uniformly across the entire flow section (Dey & Nath, 2010). Generally, blowing has been found to decrease skin friction through modification of the mean shear at the surface. Typically, these studies focus on modifications to turbulent boundary layers, although channel flow studies have been conducted using direct numerical simu-

lation at relatively low Reynolds numbers (Vigdorovich & Oberlack, 2008) with the blowing found to enhance the turbulent motions and increase Reynolds shear stress.

In comparison to the quantity of research focused on roughness effects and blowing effects on turbulent wall-bounded flow, there have been relatively few examining their combined effects (Healzer *et al.*, 1974; Schetz & Nerney, 1977; Voisinet, 1979; Holden *et al.*, 1988). Of these, only those of Healzer *et al.* (1974) and Schetz & Nerney (1977) were performed in subsonic flow. Furthermore, prior studies limited there investigations to mean flow properties, with only limited turbulence data available.

Here we present the results of experiments conducted to further our understanding of the modification made to the structure of a turbulent wall-bounded flow caused by the interaction between surface roughness and blowing boundary conditions. To perform this study, a turbulent channel flow wind tunnel was modified to introduce surface roughness and flow injection boundary conditions within its test section and the turbulent statistics measured for this flow under a range of Reynolds numbers and blowing ratios for a single, geometrically simple, surface roughness. The statistics measured for a rough surface with and without additional blowing are compared to those made for a smooth surface.

Experiment Description

The experiments were conducted in the newly constructed Turbulent Channel Flow Facility (TCFF) at the University of Kentucky Experimental Fluid Dynamics Lab (EFDL). The channel has a half height of $h = 50.8$ mm) and an aspect ratio of 9:1 to ensure quasi-2D flow at the centerline (Zanoun *et al.*, 2003). The TCFF is powered by a 5.2 kW centrifugal blower which drives the flow through conditioning, development and test sections at area averaged velocities up to $U_b = 30$ m/s; producing Reynolds numbers up to $Re_h = hU_b/\nu = 102,000$ (where U_b is the bulk velocity) or $Re_\tau = hu_\tau/\nu = 4200$.

For this set of experiments, the top surface of the TCFF test section was replaced with a nominally 2-D, sinusoidal roughness, which has a streamwise wavelength of $\lambda_x = 7$ mm and an amplitude of $k = 1$ mm. The surface had micro-cracked pores distributed uniformly along the surface and allowed for even blowing across surface introduced by a centrifugal blower forcing air through a flow conditioning apparatus. To characterize the ratio of injected to advected momentum, we define a dimensionless blowing rate of $BR = (U_{inj})/(U_m)$ where U_m is the maximum mean velocity in the channel and U_{inj} is the area-averaged velocity through the surface.

Wall-normal profile data was acquired with a single component HWA probe whose signal was digitized at 60 kHz with the acquisition time, T, for each run adjusted for each Reynolds number to capture at least 100 instances of the largest structures (which have been found to be $\mathcal{O}(20h)$, (Hutchins *et al.*, 2009)) in order to ensure converged statistics. Wall normal profiles were constructed by accurately traversing the probe to within the trough of the roughness element $80\lambda_x$ from the test section inlet. Although the exact location of the surface relative to the probe was not known, rough-walled turbulence is commonly displaced by a zero-plane displacement height, y_0, typically less than one roughness height, k. As y_0 can be determined *a posteriori*, it was therefore not essential to accurately determine the exact wall distance as all probes were traversed below the roughness height.

Direct measurement of friction velocity, U_τ, was not possible in the present case due to absence of fully-developed flow conditions. Therefore, for this set of experiments, the so-called "Clauser chart" method was used to determine the friction velocity. This method has precedence in rough-walled turbulent boundary layers (see for example Perry & Li (1990); Flack *et al.* (2004); Schultz & Flack (2007)), but has been noted to lack agreement with other methods (Akinlade *et al.*, 2004). This has resulted in multiple improvements upon the basic Clauser method (Akinlade *et al.*, 2004). However, the structure of any of these methods relies on universality of the velocity-defect law. We employed a similar method to that of Perry & Li (1990). The procedure is iterative and begins by plotting U/U_{cl} vs. $log(YU_{cl}/\nu)$ to determine $Y = y + y_0$, where U_{cl} is the channel mean centerline velocity. We have modified the method described in Perry & Li (1990) by utilizing the streamwise Reynolds stress to determine y_0 for lower Reynolds number cases, but at higher Re_τ it was assumed that the log region in the mean flow was large enough to fit the profiles accurately using equation 1 with $\kappa = 0.39$ and $B = 4.42$ (Nagib & Chauhan, 2008).

Experiments were conducted for a range of Re_τ from 650 to 7000, and BR from 0 to 0.16% and compared to smooth-walled measurements at Re_τ from 650 to 4200. All cases are summarized in table 1. This table outlines two unique aspects of this data set, the high Reynolds number achieved with roughness present in a channel flow, and the matched blowing rates across multiple Reynolds numbers.

Results and Discussion

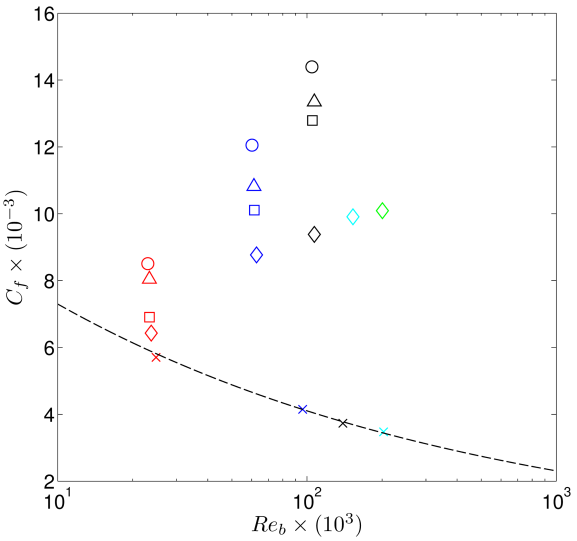

Figure 1. Coefficient of friction as a function of bulk Reynolds number. Dashed black line indicates the correlation of Dean (1978), $0.073Re_b^{-0.25}$ (with Re_b based on full channel width), solid blue line is the viscous sublayer ($U^+ = y^+$) and the log-law with constants $\kappa = 0.39$ and $B = 4.42$. Symbols indicate wall condition, (×); smooth wall cases, (◇); $BR = 0$ %, (□); $BR = 0.1$ %, (△); $BR = 0.13$ %, (○); $BR = 0.16$ %. Color indicates Reynolds number, $Re_\tau \approx 700$; red, $Re_\tau \approx 2000$; blue, $Re_\tau \approx 4000$; black, $Re_\tau \approx 5000$; cyan, $Re_\tau \approx 7000$; green

Table 1. Nominal parameters for experimental test cases

Run Parameters	U_{cl} (m/s)	Re_h	U_τ (m/s)	Re_τ	$\dot{V}_{inj}$ (SCFM)	$BR(\%)$	T (sec)
Rough Surface and Blowing Cases	4.02	13,500	0.2-0.22	672-740	0-15.92	0, 0.1, 0.13, 0.16	220
	10.6	36,000	0.62-0.7	2078-2337	0-36.6	0, 0.1, 0.13, 0.16	200
	18.5	62,000	1.09-1.32	3665-4438	0-65	0, 0.1, 0.13, 0.16	90
	26.3	88,000	1.6	5379.2	0	0	90
	34.4	115,000	2.2	7127.5	0	0	90
Smooth Wall Cases	4.2	14,100	0.197	662	0	0	220
	15.9	53,500	0.651	2189	0	0	220
	23.0	77,300	0.895	3009	0	0	100
	33.4	112,340	1.258	4229	0	0	90

The variation of friction coefficient, $C_f = \tau_w/(\rho\langle U\rangle^2)$ is presented in figure 1 as a function of the bulk Reynolds number, $Re_b = \langle U\rangle h/\nu$, where $\langle U\rangle$ is the area averaged velocity determined from $Y = 0$ to h_m, the location of maximum velocity, U_m, in the channel. This accounts for the slight asymmetry in the mean velocity profile that was observed with non-zero BR. Generally, this asymmetry was small, with h_m found to be within 2 % of h. For the non-blowing cases with roughness, the deviation of C_f from the smooth wall behavior follows typical transitional behavior, with the highest Reynolds numbers indicating an approach to fully rough conditions. Interestingly, for non-zero BR, the skin friction was observed to increase with increasing BR and the Reynolds number behavior of C_f is similar to that expected for increasing roughness. This is in contrast to results from smooth-wall studies with blowing and the turbulent boundary layer roughness and blowing results of Schetz & Nerney (1977); Voisinet (1979), where any amount of flow injection was observed to result in a reduction in skin friction when roughness was present. One potential explanation for this deviation from prior results is the nominally two-dimensional nature of the roughness used in the current study. Whereas the prior studies investigated three-dimensional roughness, the two-dimensional roughness can be expected to be composed of relatively spanwise-coherent shear-layers separating from the roughness elements. Additional blowing could then be disrupting these shear layers, resulting in enhanced momentum transfer with the surface. Alternatively, the deviation from prior studies could be due to the confined-nature of the channel-flow geometry, additional mass injection can be expected to slightly increase the adverse pressure gradient and hence the pressure drop.

The inner-scaled streamwise mean velocity profiles of all cases listed in table 1 are presented in figure 2. As expected due to the method used to obtain, U_τ, the roughness and blowing also do not appear to significantly affect the log-region in the flow. Even up to the highest Reynolds numbers, which have an essentially non-existent viscous sublayer, there is still a well defined log-layer. Focusing first on the roughness only cases, the profiles show the expected increase in ΔU^+ with increasing Reynolds number and corresponding wall shear stress, as described by equation 1. Furthermore, corresponding to the C_f behavior, additional

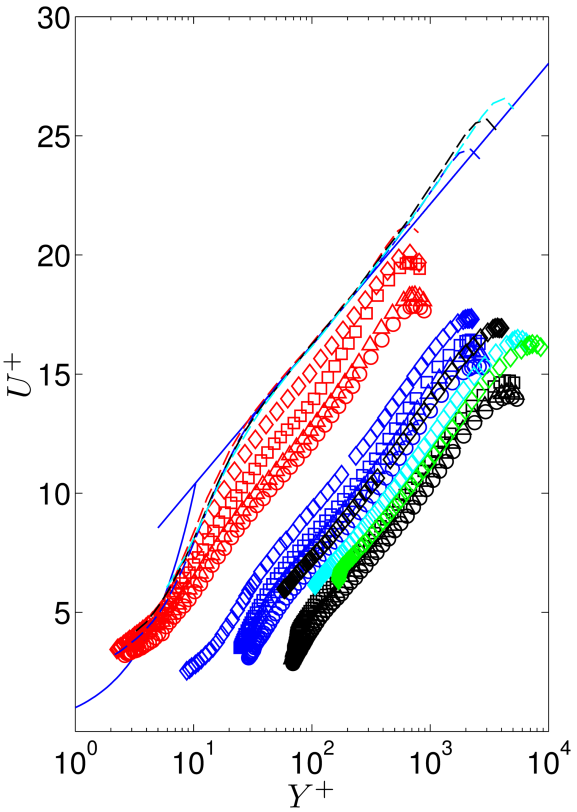

Figure 2. Streamwise mean velocity plotted in inner coordinates. Symbols indicate wall condition, (−−); smooth wall cases, (◇); $BR = 0$ %, (□); $BR = 0.1$ %, (△); $BR = 0.13$ %, (○); $BR = 0.16$ %. Color indicates Reynolds number, $Re_\tau \approx 700$; red, $Re_\tau \approx 2000$; blue, $Re_\tau \approx 4000$; black, $Re_\tau \approx 5000$; cyan, $Re_\tau \approx 7000$; green

blowing at fixed Reynolds number causes an increase ΔU^+. Thus, for the mean flow, the impact of blowing is equivalent to an effective increase in roughness.

To further explore the dependence of ΔU^+ on BR and roughness Reynolds number k^+, this quantity is presented in figure 3. Figure 3(a) shows the results spanning a wide range of k^+ values from 13 to 145 and indicate flows which follow the same trend as the sandgrain roughness of Prandtl

& Schlichting (1934). As mentioned previously, an increase in BR results in an increase in ΔU^+, analogous to an increase in roughness. However, these results show that this effective increase due to BR does not simply act as an increase in roughness height, k^+, but instead follows separate $\Delta U^+(k^+)$ trends for each BR, consistent with an effective change in roughness geometry. However, as shown in figure 3(b), it was found that a simple empirical correction of

$$\Delta U^+_{corrected} = \Delta U^+(1 - BR) \tag{2}$$

resulted in collapse of the BR data to a single roughness function.

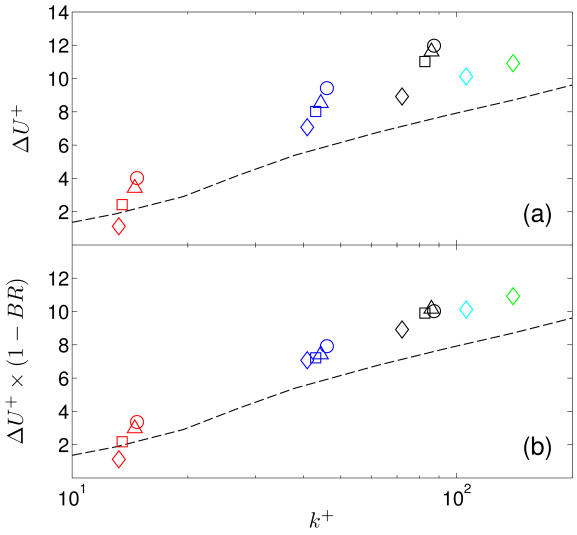

Figure 3. Roughness function plotted with respect to the roughness Reynolds number, k^+, (a) with no correction and (b) with blowing correction. The dotted line is the sand-grain roughness results from Prandtl & Schlichting (1934), symbols as in figure 2

In figure 4, the wall-normal profiles of inner scaled streamwise Reynolds stress, $\overline{u^2}^+$, corresponding to the mean velocity profiles of figure 2 are presented. Note that the highest Reynolds number cases can be expected to be subject to spatial filtering Hutchins *et al.* (2009) which will artificially reduce the magnitude of the measured streamwise Reynolds stress. Spatial filtering effects can generally be considered to be minimal for $\ell^+ = \ell U_\tau/\nu \approx 20$ (Ligrani & Bradshaw, 1987), which is the case for the two lowest Reynolds numbers in the current study. For the higher Reynolds number cases, spatial filtering effects can be considered to be confined to the near wall region (Smits *et al.*, 2011) and, in this region we will limit our analysis to a comparison between cases at similar Reynolds numbers.

Examination of figure 4 reveals that the effects of blowing on $\overline{u^2}^+$, as demonstrated by the collapse of the profiles measured at the same Reynolds number, independent of BR. This would seem to indicate that the blowing has little effect on the outer flow except as enacted through U_τ. Figure 4 also shows that the roughness in general acts to suppress the relative magnitude of the near wall peak compared to the smooth-walled cases. Furthermore, with increasing Reynolds number, the near-wall peak moves away from the

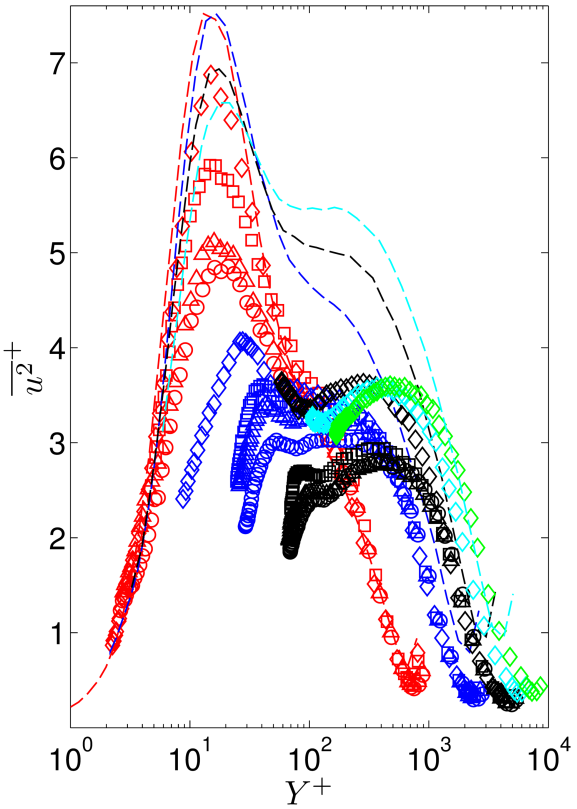

Figure 4. Inner scaled Reynolds stress, symbols as in figure 2

wall in inner units, consistent with the peak being associated with the physical scale of the roughness elements, rather than the viscous length, ν/U_τ. The non-zero BR cases exhibit similar trends with increasing BR to that of increasing roughness, consistent with the observation from the mean flow that increasing BR effectively increases the roughness.

The roughness and BR behavior of $\overline{u^2}^+$ is therefore similar to that of the mean velocity profiles, which followed the behavior predicted by Townsend's hypothesis. Given that the relative roughness height is $h/k = 51$, larger than the value noted by Jiménez (2004) of $h/k > 40$, we would expect that the effect of roughness should be confined to the inner layer and thus for wall-similarity to hold for the Reynolds stresses, as well as the mean flow. However, as indicated in figure 5, which shows the $\overline{u^2}^+$ profiles in outer coordinates, it can be observed that the results for the roughness and roughness with blowing cases do not collapse in the outer layer with the smooth-walled profiles, which collapse in this scaling for $Re_\tau \geq 3000$. Lack of collapse with the smooth-walled results is not surprising given that the flow is likely still developing over the surface in the rough-walled cases, whereas it is fully-developed for the smooth-walled cases. Close inspection of the $Re_\tau \geq 3000$ cases in figure 5 indicates that the roughness cases are self consistent in their scaling. However, as with the lower Re_τ cases, the non-zero BR cases were found to modify the turbulence well into the outer layer.

Further insight into the modification to the spatial flow structure can be gained by examining the power-spectral density calculated at each wall-normal position, pre-multiplied by the wavenumber, generated using Taylor's frozen flow hypothesis. These results are presented for the rough surface without blowing for the $Re_\tau \approx 700$

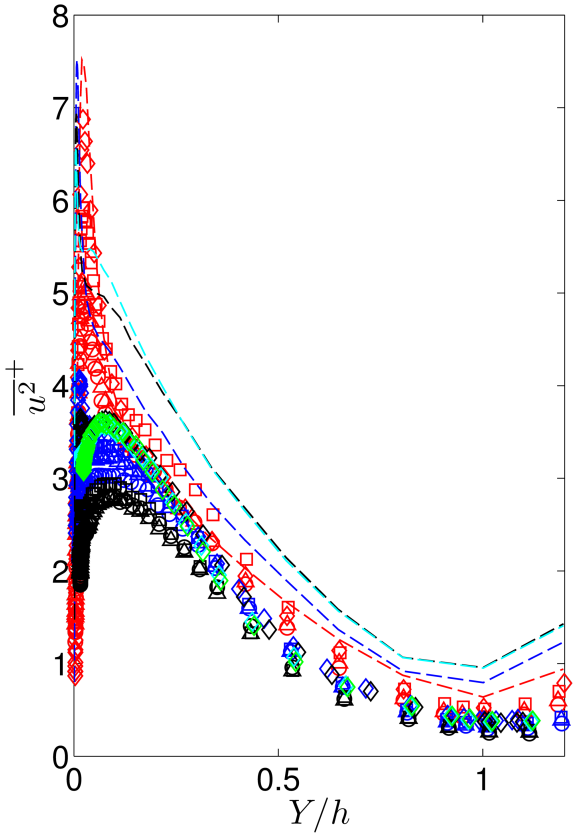

Figure 5. Outer scaled Reynolds stress, symbols as in figure 2

and 2200 cases in figures 6(a) and 7(a) respectively as spectral maps (Hutchins & Marusic, 2007). These spectral maps illustrate the dependence of the pre-multiplied spectral energy on wall distance and wavelength, λ. These spectral maps identify the wavelengths which have the greatest contribution to $\overline{u^2}^+$ as regions of high pre-multiplied spectral content.

At the lowest Reynolds number studied, the spectral map for the rough-surface case (figure 6a) is dominated by the wavelengths which form the near wall peak in Reynolds stress, and form a maxima at $\lambda/h \approx 1$. For the higher Reynolds number cases, (represented by figures 7a) the near wall peak appears at $Y/h \approx 0.015$ and is composed of eddies with $\lambda/h \approx 0.02$. Noting that $k/h = 0.02$, this behavior is consistent with the near wall turbulence production transitioning from being driven by the wall shear and scaling with the viscous length to being driven by the roughness geometry and scaling with k.

Also evident further from the wall for the higher Re_τ cases, as shown in figure 7(a), are the signature of what Monty *et al.* (2007) has termed the "dominant energy modes". These modes have been associated with the occurrence of large and very-large scale motions (LSMs and VLSMs) (Guala *et al.*, 2006). Although also evident in the lowest Re_τ case, due to the shift of the near-wall peak to smaller wavelengths, these modes become more evident for the higher Re_τ cases and appear to be largely unaffected by the presence of roughness.

To investigate the effect of non-zero BR, the difference between the $BR = 0.1\%$ and $BR = 0\%$ spectral maps are shown in figures 6(b) and 7(b) and the difference between the $BR = 0.16\%$ and $BR = 0\%$ spectral maps shown in figures 6(c) and 7(c). For the lowest Reynolds number case (figures 6b-c), the effect of blowing appears to be largely confined to the suppression of kinetic energy of the near wall peak eddies, with increased suppression occurring with increasing BR. Also noticeable, however, is a slight increase in energy at wavelengths corresponding to k and in the outer layer, suggesting a shift towards increased influence of the roughness elements. For the higher Reynolds number cases (figures 7b-c) near the wall, the additional blowing suppresses wavelengths from k to h in scale, resulting in the decrease in $\overline{u^2}^+$ observed in figure 4. More interestingly, however, is that the decrease in $\overline{u^2}^+$ observed into the outer layer appears to be due to reduction in the strength of the LSM, suggesting that the additional blowing disrupts the formation of LSM. The VLSM wavelengths, conversely, appear unaffected by blowing.

Conclusions

The combined effects of roughness and blowing boundary conditions in turbulent channel flow were examined for a Reynolds number range of $Re_\tau = 700 - 4500$. It was observed that the addition of blowing through the surface resulted in an increase in skin friction, rather than the decrease observed in smooth-wall blowing studies. The effects of roughness on the mean velocity were found to be confined to the near wall region, and the addition of blowing was found to be analogous to an increase in roughness effects allowing for a simple empirical correction for the effects on the mean profile. Although the mean profile followed the behavior predicted by Townsend's hypothesis, the Reynolds stresses did not, and modifications to the Reynolds stress profile were observed into the outer layer. This lack of scaling was found to be associated with the suppression of LSM wavelengths with increased blowing through the rough surface, which occurred simultaneously with the suppression of the near wall peak in Reynolds stress.

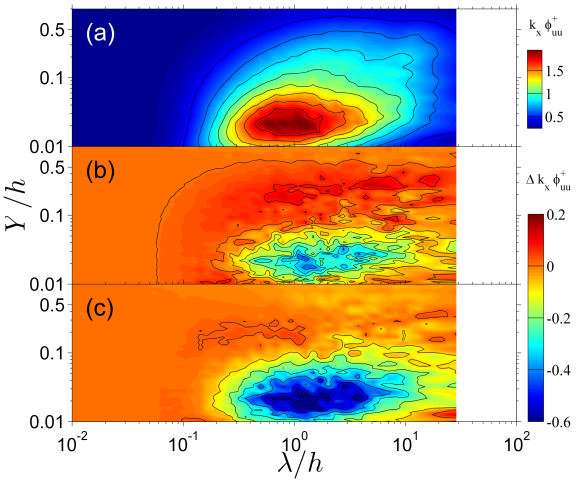

Figure 6. Premultiplied power spectra results for $Re_\tau \approx 700$. (a) Spectral maps of $k_x\phi^+_{uu}$ for roughness only case; and the contours of $\Delta\left(k_x\phi^+_{uu}\right)$ for (b) $BR = 0.1 - BR = 0$, (c) $BR = 0.16 - BR = 0$

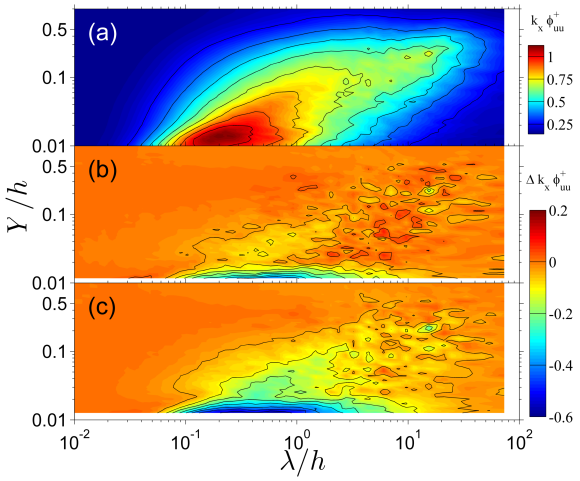

Figure 7. Premultiplied power spectra results for $Re_\tau \approx 2000$. (a) Spectral maps of $k_x\phi^+_{uu}$ for roughness only case; and the contours of $\Delta\left(k_x\phi^+_{uu}\right)$ for (b) $BR = 0.1 - BR = 0$, (c) $BR = 0.16 - BR = 0$

Acknowledgements

This work was supported by a NASA Office of the Chief Technologist's Space Technology Research Fellowship (grant number NNX12AN20H) and by Commonwealth of Kentucky funding in association with a NASA EPSCoR award (grant number NNX10AV39A).

REFERENCES

Akinlade, O.G., Bergstrom, D.J., Tachie, M.F. & Castillo, L. 2004 Outer flow scaling of smooth and rough wall turbulent boundary layers. *Experiments in Fluids* **37**, 604–612.

Çuhadaroğlu, Burhan, Akansu, Yahra Erkan & Ömür Turhal, Ahmet 2007 An experimental study on the effects of uniform injection through one perforated surface of a square cylinder on some aerodynamic parameters. *Experimental Thermal and Fluid Science* **31**, 909–915.

Dean, R.B. 1978 Reynolds number dependence of skin friction and other bulk flow variables in two-dimensional rectangular duct flow. *ASME J. Fluid Eng.* **100**, 215.

Dey, Subhasish & Nath, Tushar K. 2010 Turbulence characteristics in flows subjected to boundary injection and suction. *Journal of Engineering Mechanics* **136(7)**, 877–888.

Flack, Karen A., Schultz, Michael P.l & Shapiro, Thomas A. 2004 Experimental support for townsends reynolds number similarity hypothesis on rough walls. *Physics of Fluids* **17**, 035102.

Guala, M., Hommema, S. E. & Adrian, R. J. 2006 Large-scale and very-large-scale motions in turbulent pipe flow. *J. Fluid Mech.* **554**, 521–542.

Healzer, James Marvin, Moffat, R.J. & Kays, W.M. 1974 The turbulent boundary layer on a rough, porous plate: experimental heat transfer with uniform blowing. *Tech. Rep.* HMT-18. Stanford University CA Thermosciences Division.

Holden, M.S., Bergman, R., Harvey, J., Duryea, G. & Moselle, J. 1988 Studies of the structure of attached and separated regions of viscous/inviscid interaction and the effects of combined surface roughness and blowing in highe reynolds number hypersonic flows. *Tech. Rep.* CUBRC-88682. Calspan UB Research Center Buffalo NY.

Hutchins, N. & Marusic, I. 2007 Large-scale influences in near-wall turbulence. *Phil. Trans. R. Soc. A* **365**, 647–664.

Hutchins, N., Nickels, T. B., Marusic, I. & Chong, M. S. 2009 Hot-wire spatial resolution issues in wall-bounded turbulence. *Journal of Fluid Mechanics* **635**, 103–136.

Jiménez, J. 2004 Turbulent flows over rough walls. *Annu. Rev. Fluid Mech.* **36**, 173–196.

Krogstad, Per-Åge & Kourakine, Anatoli 2000 Some effects of localized injection on the turbulence structure in a boundary layer. *Physics of Fluids* **12(11)**, 2990–2999.

Ligrani, P. M. & Bradshaw, P. 1987 Spatial resolution and measurement of turbulence in the viscous sublayer using subminiature hot-wire probes. *Exp. Fluids* **5** (6), 407–417.

Monty, J. P., Stewart, J. A., Williams, R. C. & Chong, M.S. 2007 Large-scale features in turbulent pipe and channel flows. *J. Fluid Mech.* **589**, 147–156.

Nagib, Hassan M. & Chauhan, Kapil A. 2008 Variations of von kármán coefficient in canonical flows. *Physics of Fluids* **20**, 101518.

Perry, A.E. & Li, J.D. 1990 Experimental support for the attached-eddy hypothesis in zero-pressure gradient turbulent boundary layers. *Journal of Fluid Mechanics* **218**, 405.

Prandtl, L. & Schlichting, H. 1934 Das wiederstandagesetz rouher platten. *Werft Reederer Hafen* **15**, 1–4.

Raupach, M. R., Antonia, R.A. & Rjagopalan, S. 1991 Rough-wall turbulent boundary layers. *Appl. Mech. Rev.* **44**, 1–25.

Schetz, Joseph A. & Nerney, Brian 1977 Turbulent boundary layer with injection and surface roughness. *AIAA Journal* **15.9**, 1288–1294.

Schultz, M.P. & Flack, K.A. 2007 The rough wall-turbulent boundary layer from the smooth to the fully rough regime. *J. Fluid Mech.* **580**, 381–405.

Smits, A. J., Monty, J. P., Hultmark, M., Bailey, S. C. C., Hutchins, N. & Marusic, I. 2011 Spatial resolution correction for wall-bounded turbulence measurements. *J. Fluid. Mech* **676**, 41–53.

Townsend, A. A. 1976 *The Structure of Turbulent Shear Flow*. Cambridge, UK: Cambridge University Press.

Vigdorovich, Igor & Oberlack, Martin 2008 Analytical study of turbulent poiseuille flow with wall transpiration. *Physics of Fluids* **20**, 055102.

Voisinet, R.L.P. 1979 Influence of roughness and blowing on compressible turbulent boundary layer flow. *Tech. Rep.*. Naval Surface Weapons Center, White Oak Lab, Silver Spring, MD.

Zanoun, E. S., Durst, F. & H., Nagib. 2003 Evaluating the law of the wall in two-dimensional fully developed turbulent channel flows. *Phys. Fluids* **15**, 3079–3089.